Crystalline Oxides on Silicon: The First Five Monolayers

R. A. McKee, F. J. Walker, and M. F. Chisholm
Oak Ridge National Laboratory, Oak Ridge, Tennessee 37831-6118
(Received 8 June 1998)

The long-standing problem of growing a commensurate crystalline oxide interface with silicon has been solved. Alkaline earth and perovskite oxides can be grown in perfect registry on the (001) face of silicon, totally avoiding the amorphous silica phase that ordinarily forms when silicon is exposed to an oxygen containing environment. The physics of the heteroepitaxy lies in establishing a sequenced transition that uniquely addresses the thermodynamics of a layer-by-layer energy minimization at the interface. A metal-oxide-semiconductor capacitor using $SrTiO_3$ as an alternative to SiO_2 yields the extraordinary result of $t_{eq} < 10$ Å. [S0031-9007(98)07238-X]

PACS numbers: 81.15.Hi, 73.40.Qv, 73.61.–r, 77.55.+f

Since the advent of the integrated circuit in 1959 and the introduction of metal-oxide-semiconductor (MOS) capacitors in the early 1960s, electronic technology has relied on silica (SiO_2) as the gate dielectric in a field effect transistor. However, silica-based transistor technology is approaching fundamental limits. Feature-size reduction and the ever-demanding technology roadmaps have imposed scaling constraints on gate oxide thickness to the point where excessive tunneling currents make transistor design untenable; an alternative gate dielectric is needed [1].

While now it is especially clear, with SiO_2 thicknesses in the sub-50-Å regime, the argument for alternative gate oxides is not new; it has been made from different perspectives for over 40 years [2–5]. Quite aside from the "physical" thickness limits that tunneling currents make obvious, the amorphous SiO_2 interface with silicon leaves dangling bonds as electronic defects disrupting translational symmetry at the interface. An alternative crystalline gate oxide would, in principle at least, uniquely maintain a one-to-one correspondence between physical and electrical structure preserving translational symmetry to atomic dimensions.

Crystalline oxides on silicon (COS), simply by virtue of their high dielectric constants, could fundamentally change the scaling laws for silicon-based transistor technology. More importantly COS introduces the possibility for an entirely new device physics based on utilization of the anisotropic response of crystalline oxides grown commensurately on a semiconductor. In this Letter, we report that high dielectric constant alkaline earth and perovskite oxides can be grown in perfect registry with silicon. Commensurate heteroepitaxy between the semiconductor and the oxide is established via a sequenced transition that uniquely addresses the thermodynamics of a layer-by-layer energy minimization at the interface. The perfection of the physical structure couples directly to the electrical structure, and we thus obtain the unparalleled result of an equivalent oxide thickness of less than 10 Å in a MOS capacitor.

An equivalent oxide thickness t_{eq} can be defined for a MOS capacitor as

$$t_{eq} = \varepsilon_0 \frac{\varepsilon_{SiO_2}}{(C/A)_{ox}} \tag{1}$$

in which ε_{SiO_2} and ε_0 are the dielectric constants of silica and the permittivity of free space. $(C/A)_{ox}$ is the specific capacitance of the MOS capacitor. Figure 1 shows a plot of our data for specific capacitance against voltage for a 150-Å-thick film of $SrTiO_3$ on (001) Si. The capacitor exhibits a C/A value of 40 tF/um^2 at negative voltages where the field is across the oxide. The interface trap density, obtained from the frequency dependence of the capacitance data, is sharply peaked at 0.11 eV above the valence band with values that range from 10^{10} cm^2 to 6×10^{11} cm^2. An analysis of this data suggests that the interface registry is so perfect that the original silicon surface step interactions can be identified as the interface trap states [6].

This is an unparalleled result for a MOS capacitor. In what follows, we will describe the first five monolayers of a structure transition from silicon to an ionic oxide. The sequencing of these five monolayers stabilizes the commensurate crystalline interface of a COS structure.

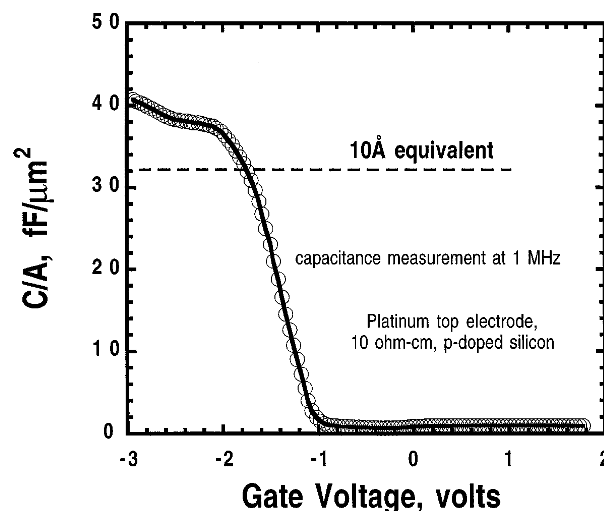

FIG. 1. Capacitance/voltage for a $SrTiO_3$/Si capacitor. The $SrTiO_3$ is 150 Å thick, and with p-type silicon the capacitance of the oxide is obtained with silicon in accumulation at negative voltages.

 0031-9007/98/81(14)/3014(4)$15.00 © 1998 The American Physical Society

Figure 2 provides an overview of the heteroepitaxy and oxide registry on (001) Si looking down Si[110]. The cross section in Fig. 2 was obtained using Z-contrast electron microscopy [7,8] to obtain a direct structure image from a film grown 3 unit cells thick and then overcovered with amorphous silicon. The structure [inset in the left; oxygen atoms are not shown] shows strontium ions in the simple perovskite $SrTiO_3$, against silicon with titanium ions in the perovskite cube center, one row up. The covalently bonded silicon atoms are shown in the dumbbell projection. This 3-unit-cell film will be used to describe the details of the interface structure in subsequent discussions. The data in Fig. 1 were obtained by continuing growth on such a structure to 150 Å total thickness. Molecular beam epitaxy methods were used to prepare the thin films [9]. Heteroepitaxy was obtained by expressly considering the energetics of layer-by-layer stabilization.

Layer-by-layer interfacial energy minimization, as a heteroepitaxy concept, was first introduced experimentally by McKee *et al.* [10] in a study of heteropitaxy between MgO and $BaTiO_3$. This concept has recently been developed computationally in a paper by Sayle, Catlow, and Perrin [11]. In the original experimental study of the MgO/$BaTiO_3$ layering energetics, it was shown that commensurate heteroepitaxy could be obtained only if interfacial electrostatics was satisfied in the layering sequence. The interfacial energetics of semiconductor/oxide systems is exactly analogous.

A number of reported attempts to grow oxide structures on silicon have been made [12–15], but until now there has been no definitive proof that a commensurate crystalline oxide-on-silicon interface could be obtained. While recent years have seen extensive studies of the synthesis of layered compounds with examples in superconductivity [16–18], giant magnetoresistance [19–21], and ferroelectricity [22,23], there has been very little clarity regarding the energetics of heteropitaxial stability at a semiconductor/oxide interface.

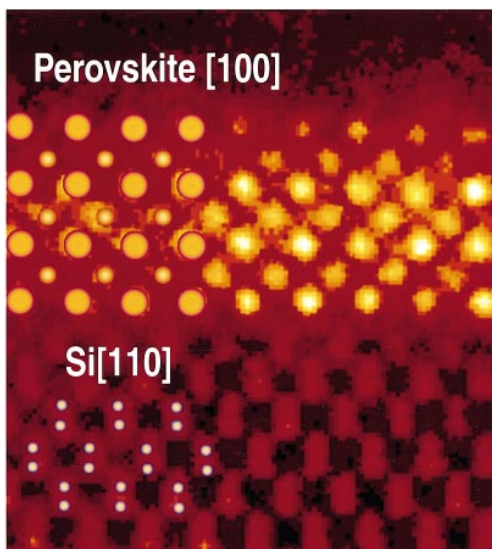

FIG. 2(color). Z-contrast image of $SrTiO_3$ on (001) silicon. The epitaxy that is apparent is (001) $SrTiO_3$ ∥ (001) Si and $SrTiO_3$[110] ∥ Si[100]. In the left side of the parallel image is an inset model of the perovskite/silicon projection.

In an attempt to establish candidate materials for an oxide interface with silicon, Hubbard and Schlom [24] have examined the thermodynamics of binary oxides of every element in the period table. While their study was a phenomenological treatment which ignored any question of heteroepitaxy, they concluded that the alkaline earth oxides would be thermodynamically stable against silicon as binary oxides, but were unable to identify any ternary oxides as a candidate. However, the $SrTiO_3$/silicon interface shown in Fig. 2 is physical evidence that a ternary oxide in the perovskite class, at least, is stable against silicon. The basis for this stability lies in the context of metal oxide-dominant, 3-component phase equilibria [25].

The phase equilibria for a 3-component, metal-Si-O system can be considered to be metal oxide dominant or SiO_2 dominant. The "dominance" is based on the configuration of stable tie lines between components of a 3-component phase diagram. While all of the transition metals in perovskite oxides are SiO_2 dominant, the thermodynamic data [26] for the A-Si-O ternary systems show that all of the alkaline earth metals A form silicides and are metal-oxide dominant. Therefore heteroepitaxial growth of oxides on silicon cannot be simply initiated with the oxide layer. The total system energy for perovskite heteroepitaxy on silicon must include the stable ASi_2/AO interface. The silicide layer at this interface can be as thin as 1 ML.

These ideas have been systematically tested with molecular beam epitaxy methods. Starting from a reconstructed (001) Si surface and a growth temperature of 850 °C, exposure of the silicon surface to an alkaline earth metal (for example, barium or strontium) leads to a series of submonolayer ordered structures. Figure 3 is a data set taken from coverage-dependent, reflection high-energy electron diffraction (RHEED) intensity oscillation of the specular 0,0 rod at the Si[110] zone axis. The ordered structure at $\frac{1}{4}$ monolayer (ML) is a centered (4×2) structure that is highly perfect and is commensurate with silicon. It is stable on cooling to room temperature and reheating. X-ray photoelectron spectroscopy data from this surface shows it to be shifted in binding energy to a "silicide" electronic structure. As we will demonstrate, this structure is not an adsorbed state but rather is a $c(4 \times 2)$ silicide in which the alkaline earth metal has replaced and displaced silicon atoms in the top surface. Unlike the incommensurate, orthorhombic silicide that forms if the surface exposure is continued past 1 ML, this silicide is fully commensurate and thermodynamically stable, and remains at the interface as part of the overgrowing perovskite structure. High temperature is required for its formation; this commensurate silicide structure will not form if alkaline earth metals are deposited at low temperatures on a reconstructed (001) Si and subsequently

heated to a higher temperature. Understanding this step in the growth sequence is critical. This silicide layer is the second monolayer in the COS interface having followed the reconstructed oxide-free (2×1) silicon surface on (001) Si.

The third, fourth, and fifth monolayers of the COS interface are all grown at 200 °C with oxygen being introduced between the third and fourth layers. By covering the silicide with an alkaline earth metal to $\frac{1}{2}$ ML at low temperatures, the critical step of oxygen introduction can be accomplished without perturbing the silicide layer. At the third monolayer, oxygen in codeposition with strontium forms SrO in thermodynamic equilibrium with the underlying silicon/silicide interface. While SrO will strain to the 3.84 Å [110] planar spacing of silicon, it can be alloyed during growth with barium to obtain a perfectly strain free BaSrO. The final two layers in our five monolayer structure are either repeats of the AO layers to form 1 unit cell of a NaCl-type oxide structure or the transition metal oxide layer followed by another AO layer to form the perovskite structure. This latter process was repeated to a total of 3 unit cells to obtain the Z-contrast image in Fig. 2.

The final part of this Letter is a description of the $c(4 \times 2)$ silicide that is the key to the commensurate stability of this COS structure on silicon. Figure 4 contains two Z-contrast images of the 3-unit-cell perovskite/silicon interface looking down the $\langle 110 \rangle$ direction of silicon and a plan view construction of the interface silicide registry looking parallel to Si[001]. The two images labeled (a) and (b) are obtained from the same cross section but from positions along the interface that have relative displacements along the $\langle 001 \rangle$ surface normal that differ by odd multiples of $a_{\mathrm{Si}}/4$. This allows orthogonal views of the interface to be observed in domains separated by, for example, a single-height surface step, a convenience that is a result of the twofold rotation axis about Si[001].

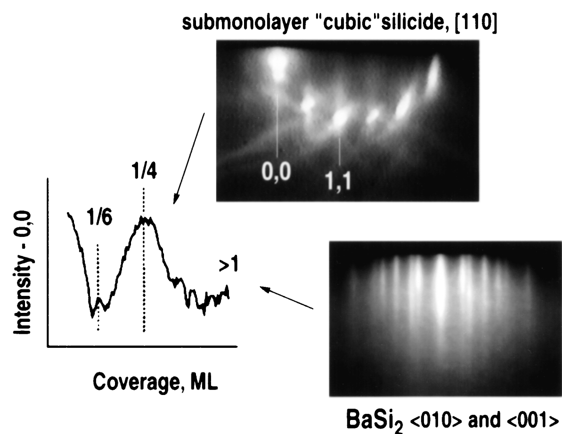

FIG. 3. Submonolayer intensity oscillation as a function of coverage. Upper center, RHEED pattern at [110] for $\frac{1}{4}$ ML, rotated a few degrees off-asymuth; the specular spot from which the intensity modulation is observed is the larger of the two spots at 0,0. Lower right, RHEED pattern just past 1 ML showing variants of orthorhombic $BaSi_2$.

From these images it is possible to construct the interface registry for the silicide layer between the perovskite and silicon. The analysis of the images is drawn in plan view in the bottom panel of Fig. 4. From the RHEED data described in Fig. 3, the initial silicide growth developed with a $c(4 \times 2)$ diffraction pattern, but it is not possible to determine from RHEED alone whether that pattern is

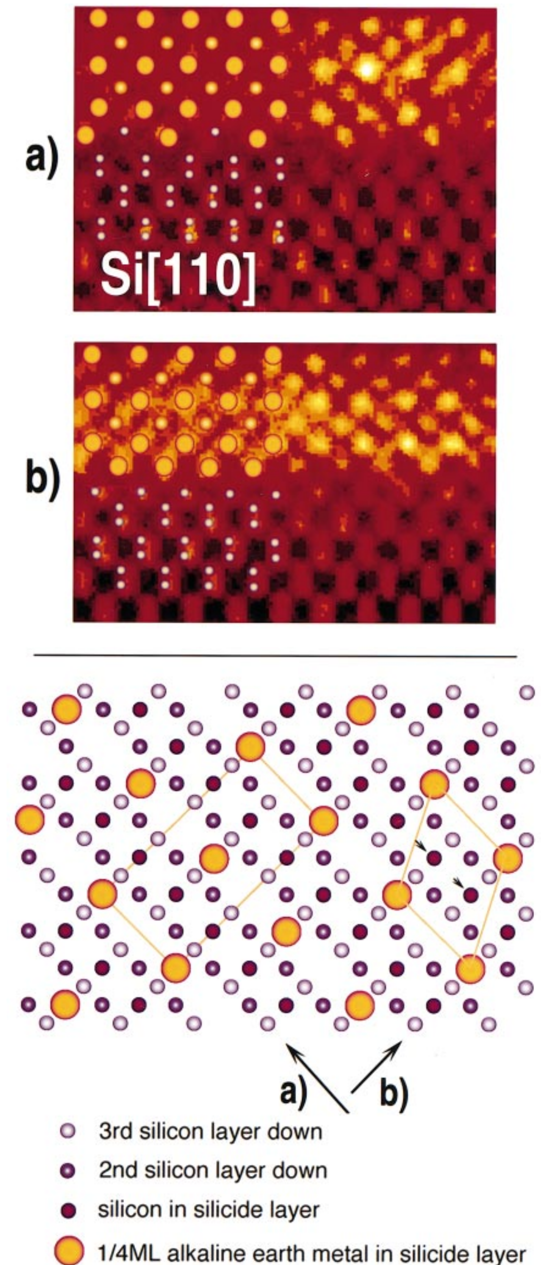

FIG. 4(color). Strontium silicide interface model as deduced from Si[110] images assuming the $SrSi_2$ composition. Panels (a) and (b) are Z-contrast cross-sectional images that provide orthogonal views of the interface. The bottom panel is a schematic plan view of the silicide—the arrows a and b identify the viewing direction of panels (a) and (b). The small arrows show the $\frac{a}{4}[110]$ displacement of the silicide layer relative to the silicon layer it replaces. A crystallographically equivalent variant of this silicide can be produced by a 90° rotation about Si[001].

from an absorbate ordering or whether a surface silicide has formed. The thermodynamics argues for a silicide between the *A*O plane of the perovskite and silicon.

In the plan view surface registry (the bottom panel of Fig. 4), the direction labeled "*a*" reflects the direction imaged in panel (a); "*b*" provides the orthogonal view obtained from panel (b). It is apparent from this analysis that the silicide layer is indeed at the interface; the top layer of the silicon truncation is dramatically reordered. Moreover, its symmetry is $c(4 \times 2)$ as was indicated in the RHEED pattern in Fig. 3.

In panel (a) the Z contrast shows a "bright/dim" sequence at the interface with double the silicon periodicity. The model inset in the left of panel (a) and also in the surface registry construction below panel (b) shows that this bright/dim sequence is due to the periodicity of strontium in the silicide layer; every other atomic row is occupied. By observing the 90° rotation in panel (b), the intensity sequence is now bright/bright; i.e., every row is occupied by strontium. These observations establish the $c(4 \times 2)$ symmetry of the interfacial silicide.

The $\langle 110 \rangle$ projections in panels (a) and (b) allow us to fix the strontium/silicon ratio as 1 to 2 or 1 to 3. Occlusion of the silicon site between the strontium atoms in the a projection prevents a discrimination; the disilicide would require that there be no silicon in the strontium rows parallel to a. The images unequivocally provide evidence that strontium atoms have substituted for silicon and the silicide layer is displaced relative to the silicon lattice by an $a/4[110]$ glide.

The interface is substantially different from simply an absorbed surface ordering; a silicide structure has formed. As stated in the thermodynamic discussion, the layer energy minimization requires an alkaline earth silicide layer between the alkaline earth oxide plane of the perovskite oxide and the underlying silicon. The silicide reaction and ordering presented in Fig. 3 is preserved after the subsequent perovskite oxide is grown on silicon, as Fig. 4 clearly shows.

We have established that an energy minimization consistent with a layer-by-layer thermodynamic stability argument is required for commensurate heteroepitaxy to develop at a semiconductor/oxide interface. This is the first time that a crystalline oxide has been obtained as a monolithic, commensurate structure on silicon. Experimental measurements of the electrical properties of this interface with a 150 Å overgrowth of $SrTiO_3$ show conclusively that alternative gate oxides are possible. A MOS capacitor with an equivalent oxide thickness of less than 10 Å is obtained and clearly demonstrates that COS offers the opportunity for a fundamental change in device physics for semiconductor technology.

We would like to express appreciation to Ron Feenstra and Chong Long Fu for careful reading of this manuscript and to acknowledge that joint support of the Laboratory Directed Research and Development Program of Oak Ridge National Laboratory and the Division of Materials Sciences, U.S. Department of Energy, under Contract No. DE-AC05-96OR22464 with Lockheed Martin Energy Research Corporation.

[1] L.C. Feldman, E.P. Gusev, and E. Garfunkel in *Fundamental Aspects of Ultrathin Dielectrics on Si-based Devices,* edited by E. Garfunkel *et al.* (Kluwer, Dordrecht, 1998).
[2] D.H. Looney, U.S. Patent No. 2,791,758 (1957); J.A. Morton, U.S. Patent No. 2,791,761 (1957); I.M. Ross, U.S. Patent No. 2,791,760 (1957); W.L. Brown, U.S. Patent No. 2,791,759 (1957).
[3] J.D. Meindl, J. Vac. Sci. Technol. **14**, 192 (1996).
[4] *National Technology Roadmap for Semiconductors* (Sematech Corp., San Jose, CA, 1997).
[5] Cem Basceri, S.K. Streiffer, A.I. Kingon, and R. Waser, J. Appl. Phys. **82**, 2497 (1997).
[6] R.A. McKee, F.J. Walker, and M.F. Chisholm (unpublished).
[7] D.E. Jesson and S.J. Pennycook, Proc. R. Soc. London A **249**, 272 (1995).
[8] M.F. Chisholm, A. Maiti, S.J. Pennycook, and S.T. Pantelides, Phys. Rev. Lett. **80**, 132 (1998).
[9] R.A. McKee, F.J. Walker, J.R. Conner, E.D. Specht, and D.E. Zelmon, Appl. Phys. Lett. **59**, 782 (1991).
[10] R.A. McKee, F.J. Walker, E.D. Specht, G.E. Jellisen, and L.A. Boatner, Phys. Rev. Lett. **72**, 2741 (1994).
[11] D.C. Sayle, C.R.A. Catlow, and M.-A. Perrin, Phys. Rev. B **56**, 15 952 (1997).
[12] Y. Kado and Y. Arita, J. Appl. Phys. **61**, 2398 (1987).
[13] H. Mori and H. Ishiwara, Jpn. J. Appl. Phys. **30**, L1415 (1991).
[14] T.W. Kim, Y.S. Yoon, S.S. Yom, and J.Y. Lee, Appl. Phys. Lett. **64**, 2676 (1994).
[15] M. Alexe, Appl. Phys. Lett. **72**, 2283 (1998).
[16] J.G. Bednorz and K.A. Muller, Z. Phys. B **64**, 189 (1986).
[17] J.N. Eckstein and I. Bozovic, Annu. Rev. Mater. Sci. **25**, 679 (1995).
[18] R. Feenstra, X. Li, M. Kanai, S. Kawai, J.D. Budai, E.C. Jones, Y.R. Sun, J.R. Thompson, S.J. Pennycook, and D.K. Christen, Physica (Amsterdam) **224C**, 300 (1994).
[19] S.S.S. Parkin, N. More, and K.P. Roche, Phys. Rev. Lett. **64**, 2304 (1990).
[20] Z. Trajanovic, C. Kwon, M.C. Robson, K.-C. Kim, M. Rajeswari, R. Ramesh, T. Venkatesan, S.E. Lofland, S.M. Bhagat, and D. Fork, Appl. Phys. Lett. **69**, 1005 (1996).
[21] R. Schad, D. Bahr, J. Falta, P. Belien, and Y.J. Bruynseraede, J. Phys. Condens. Matter **10**, 61 (1998).
[22] D.J. Taylor, R.E. Jones, P. Zurcher, P. Chu, Y.T. Lii, B. Jiang, and S.J. Glllespie, App. Phys. Lett. **68**, 2300 (1996).
[23] J. Lee and R. Ramesh, Appl. Phys. Lett. **68**, 484 (1996).
[24] K.J. Hubbard and D.G. Schlom, J. Mater. Res. **11**, 2757 (1996).
[25] R. Beyers, J. Appl. Phys. **56**, 147 (1984).
[26] I. Barin and O. Knacke, *Thermochemical Properties of Inorganic Substances* (Springer, Berlin, 1973-1977).